Sphingosine kinase 2 (SphK2) depletion alters redox metabolism and enhances inflammation in a diet-induced MASH mouse model

VISUAL ABSTRACT

Sphingosine kinase 2 (SphK2) depletion alters redox metabolism and enhances inflammation in a diet-induced MASH mouse model

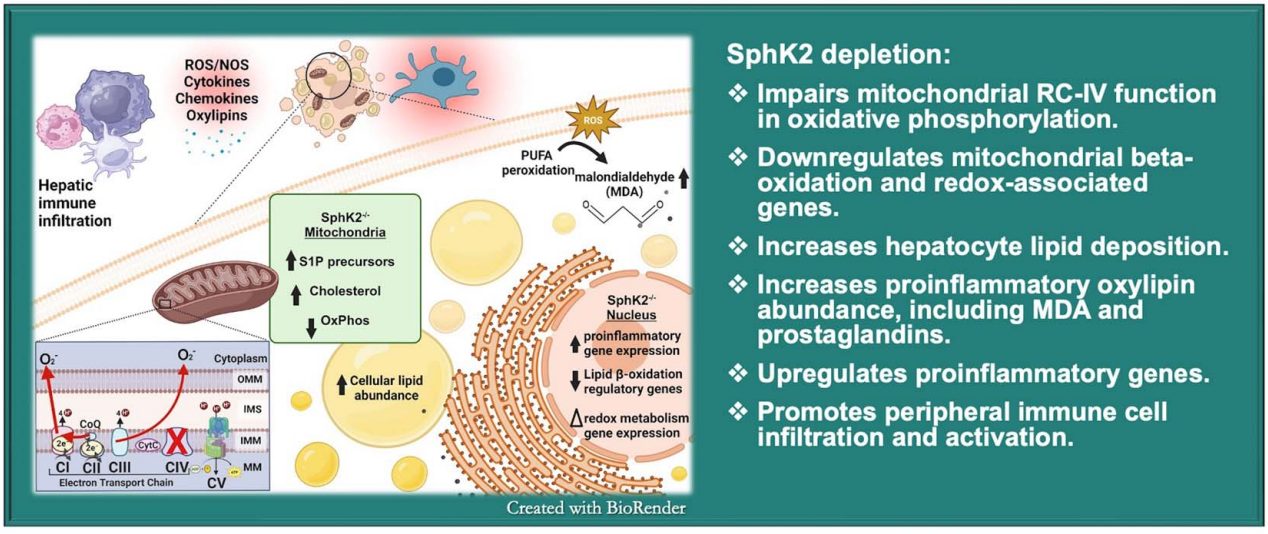

AASLD Jackson, et al. | *Hepatology Communications*. 2024. Hepatology Communications

Received: 24 June 2024 | Accepted: 15 September 2024

DOI: 10.1097/HC9.0000000000000570

ORIGINAL ARTICLE

OPEN

Sphingosine kinase 2 (SphK2) depletion alters redox metabolism and enhances inflammation in a diet-induced MASH mouse model

Kaitlyn G. Jackson[1] | Derrick Zhao[1] | Lianyong Su[1,2] | Marissa K. Lipp[1] | Cameron Toler[1] | Michael Idowu[3] | Qianhua Yan[1,4] | Xuan Wang[1] | Emily Gurley[1] | Nan Wu[1] | Puneet Puri[2,5] | Qun Chen[6,7,8] | Edward J. Lesnefsky[6,7,8] | Jeffrey L. Dupree[2,9] | Phillip B. Hylemon[1] | Huiping Zhou[1,2]

[1]Department of Microbiology and Immunology, Virginia Commonwealth University School of Medicine, Richmond, Virginia, USA

[2]Department of Research, Richmond Veterans Healthcare System, Richmond, Virginia, USA

[3]Department of Pathology, Medical College of Virginia Campus, Virginia Commonwealth University, Richmond, Virginia, USA

[4]Department of Endocrinology, Jiangsu Province Hospital of Chinese Medicine, Nanjing University of Chinese Medicine, Nanjing, China

[5]Division of Gastroenterology, Department of Internal Medicine, Hepatology, and Nutrition, Virginia Commonwealth University School of Medicine, Richmond, Virginia, USA

[6]Department of Internal Medicine, Cardiology, Pauley Heart Center, Richmond, Virginia, USA

[7]Department of Physiology and Biophysics, Virginia Commonwealth University, Richmond, Virginia, USA

[8]Department of Biochemistry and Molecular Biology, Virginia Commonwealth University, Richmond, Virginia, USA

[9]Department of Anatomy and Neurobiology, Virginia Commonwealth University, Richmond, Virginia, USA

Correspondence
Huiping Zhou, Department of Microbiology & Immunology, Virginia Commonwealth University, 1220 East Broad Street, MMRB-5044, Richmond, VA 23298-0678, USA.
Email: huiping.zhou@vcuhealth.org, huiping.zhou@va.gov

Abstract

Background: Sphingosine-1 phosphate (S1P) is a bioactive lipid molecule that modulates inflammation and hepatic lipid metabolism in MASLD, which affects 1 in 3 people and increases the risk of liver fibrosis and hepatic cancer. S1P can be generated by 2 isoforms of sphingosine kinase (SphK). SphK1 is well-studied in metabolic diseases. In contrast, SphK2 function is not well characterized. Both sphingolipid and redox metabolism dysregulation contribute to MASLD pathologic progression. While SphK2 localizes to both the nucleus and mitochondria, its specific role in early MASH is not well defined.

Methods: This study examined SphK2 depletion effects on hepatic redox metabolism, mitochondrial function, and inflammation in a 16-week

Abbreviations: BP, biological process; CDNW, control diet plus normal water; Cybb, cytochrome b-245, beta chain; CYP27, (cytochrome P450 oxidase) 27-hydroxylase; CYP7b1, cytochrome P450, family 7, subfamily B, polypeptide 1; GO, gene ontology; Hmox1, heme oxygenase-1; MDA, malondialdehyde; RC, respiratory complex; Redox, oxidation-reduction; ROS, reactive oxygen species; S1P, sphingosine-1 phosphate; Sardh, sarcosine dehydrogenase; SphK, sphingosine kinase; Tbxas1, thromboxane A synthase 1; WDSW, western diet plus sugar water; WT, wild type.

Supplemental Digital Content is available for this article. Direct URL citations are provided in the HTML and PDF versions of this article on the journal's website, www.hepcommjournal.com.

western diet plus sugar water (WDSW)-induced mouse model of early MASH.

Results: WDSW-*SphK2*$^{-/-}$ mice exhibit increased hepatic lipid accumulation and hepatic redox dysregulation. In addition, mitochondria-localized cholesterol and S1P precursors were increased. We traced *SphK2*$^{-/-}$-mediated mitochondrial electron transport chain impairment to respiratory complex-IV and found that decreased mitochondrial redox metabolism coincided with increased oxidase gene expression and oxylipin production. Consistent with this relationship, we observed pronounced increases in hepatic inflammatory gene expression, prostaglandin accumulation, and innate immune homing in WDSW-*SphK2*$^{-/-}$ mice compared to WDSW-wild-type mice.

Conclusions: These studies suggest SphK2-derived S1P maintains hepatic redox metabolism and describe the potential consequences of SphK2 depletion on proinflammatory gene expression, lipid mediator production, and immune infiltration in MASH progression.

Keywords: immune, mitochondria, oxylipin, redox, sphingosine-1 phosphate

INTRODUCTION

MASLD affects nearly 1 in 3 people in the developed world; its prevalence is expected to increase alongside other cardiometabolic disorders.[1] Approximately 30% of patients with MASLD progress to a more severe stage termed MASH, characterized by inflammation onset and varying degrees of fibrosis. Moreover, MASH increases the risk of liver cirrhosis, end-stage liver disease, and hepatic and extrahepatic cancer development.[2,3] Hepatic sphingolipid metabolism dysregulation and mitochondrial function contribute to MASLD pathogenesis.[4–7] However, the specific cellular mechanisms that drive the progression from steatosis to MASH remain unclear.

Mitochondrial dysfunction has been implicated in MASLD pathogenesis for 3 decades.[8,9] The role of mitochondria in MASLD varies according to the disease stage. In steatosis, hepatocytes initially respond to metabolic overload by increasing mitochondrial beta-oxidation, tricarboxylic acid cycle, and oxidative phosphorylation activity. Increased mitochondrial reactive oxygen species (ROS) production is noted in several studies but is initially offset by antioxidant responses.[10,11] Chronic cellular stress decreases mitochondrial beta-oxidation and overwhelms antioxidant mechanisms, leading to hepatic lipid accumulation and oxidative stress.[11] Mitochondrial dysfunction is not merely a compartmentalized source of cellular stress.[12] Instead, mitochondria should be regarded as central redox regulators; their dysfunction governs greater cellular metabolic and proinflammatory networks.[13–15] Mitochondrial processes are primarily associated with metabolic overload. However, recently, overall hepatic redox dysregulation has been strongly linked to genetic risk factors in patients with MASLD.[16]

Sphingolipids are essential for maintaining cellular membrane integrity and function as active lipid signaling molecules.[4,17] Sphingosine-1 phosphate (S1P) is one of the most well-characterized sphingolipids, and is produced by 2 sphingosine kinase (SphK) isoforms: SphK1 and SphK2. SphK1 is primarily localized to the cytosol and has been well-studied. In contrast, SphK2 contains an N-terminal lipid-binding domain that promotes its unique localization to the nucleus and mitochondria.[18,19] Previous studies demonstrate that S1P receptor 2 and SphK2 are critical lipid metabolic regulators in the liver.[20–23] SphK2-derived S1P is an endogenous histone deacetylase 1 and 2 inhibitor within the nucleus.[24] Although SphK2 is constitutively expressed in all mammalian tissues, its role in mitochondrial function and contribution to hepatic redox regulation and inflammation in MASH progression have not been thoroughly explored.[25]

This study investigates SphK2 depletion effects on mitochondrial function, gene expression, and inflammation using a western diet and sugar water (WDSW)-induced MASLD model with global SphK2 knockout

(*SphK2*$^{-/-}$) mice. Our data suggest that SphK2 depletion enhances MASH progression in WDSW-fed mice through respiratory complex-IV (RC-IV)-mediated mitochondrial dysfunction and proinflammatory and redox-associated gene expression alterations. These changes were accompanied by increased reactive oxylipin formation, proinflammatory mediator production, and hepatic immune cell recruitment.

METHODS

Human liver tissue

Liver tissues from male and female presumed healthy patients and patients with MASH (Supplemental Table S1, http://links.lww.com/HC9/B84) were obtained through the Liver Tissue Cell Distribution System, which is funded by the National Institutes of Health (Contract# HSN276201200017C).

Animal studies

Male and female (12- to 18-week-old) C57BL/6-NJ background constitutive *SphK2*$^{-/-}$ and age-matched and sex-matched wild-type (WT) male and female mice were used for this study. All mice were bred under pathogen-free conditions and housed in individually ventilated cages with 12-hour light-dark cycles. Single housing was avoided to minimize stress-associated feeding behaviors. All mice were genotyped before use. Adult mice were fed a western, high-fat diet (Envigo Rx. 356989, T.D. 88137) plus sugar water (23.1 g/L fructose, 18.9 g/L glucose; WDSW) or a control diet with similar nutrient content, plus normal water (CDNW) *ad libitum* for 16 weeks. At the study endpoint, the mice were anesthetized with isoflurane and sacrificed by exsanguination. The blood and liver were harvested after sacrifice. All procedures were approved by the AAALAC-accredited VCU IACUC committee.

RNA isolation and reverse transcription-quantitative PCR

Total RNA was isolated from whole-liver tissue using TRIzol reagent (Qiagen). RNA purity was measured using a NanoDrop UV-Vis spectrophotometer (Thermo Fisher Scientific). Reverse transcription of total RNA to cDNA was performed using a high-capacity cDNA synthesis kit (Thermo Fisher) according to the manufacturer's instructions. Quantitative PCR analysis was conducted using SYBR green-based detection on a CFX Touch Real-Time PCR detection system (Bio-Rad). All primer sequences are provided in Supplemental Table S5, http://links.lww.com/HC9/B84. Reactions were performed with hot-start Taq polymerase at 95°C for 10 minutes, followed by 40 cycles of 95°C for 15 seconds (denaturation), 55°C for 30 seconds (annealing), and 60°C for 1 minute (extension). Fluorescence quantification data were collected during the extension. The resulting Cq values were used to calculate gene expression, normalized to actin, using the Livak ($2^{-\Delta\Delta Ct}$) method.

NanoString RNA multiplex analysis

Total RNA from the same samples described in "RNA isolation and reverse transcription-quantitative PCR" was diluted to 40 ng/μL in nuclease-free water. nCounter Mouse Immunology (catalog # PSTD Mm Immunology-12) and Mouse Metabolism (XT-CSO-MMP1-12) panels were used to assess the transcriptional profile (NanoString). Rosalind software was used to determine differentially expressed genes based on statistical significance ($p < 0.05$) and fold change (± 2). The data were organized in Excel, and representative graphs were prepared in GraphPad PRISM version 10.1.2. Data from this study were deposited in the European Genomephenome Archive (EGA) under the accession code GSE280083 and GSE280101.

Additional information is described in the Supplemental Materials and Methods, http://links.lww.com/HC9/B84.

RESULTS

Decreased SphK2 is linked to liver damage in patients with MASH and a diet-induced MASH mouse model

Reduced *SphK2* mRNA levels were observed in hepatic biopsy samples from patients with MASH compared to normal, presumed healthy controls (Figure 1A). This decrease was recapitulated in mice fed WDSW for 24 weeks (Figure 1B). To further investigate SphK2 depletion effects *in vivo*, we employed a 16-week WDSW-feeding model. Based on previous studies conducted with DIAMOND mice, we selected this time point to represent the early MASH stage, where SphK2 gene effects on mitochondrial function and inflammation may be studied without extensive diet-induced effects.[26,27] Whole-body weight, liver weight, and serum chemistry were assessed. While an increase in the liver-to-body weight ratio was observed, further data stratification showed that this was due to maintained liver mass despite body weight loss (Figures 1C–F). Histological analysis, evaluated by a certified pathologist, showed no significant changes in MASLD progression (Figures 2A, B). However, a blood chemistry panel revealed

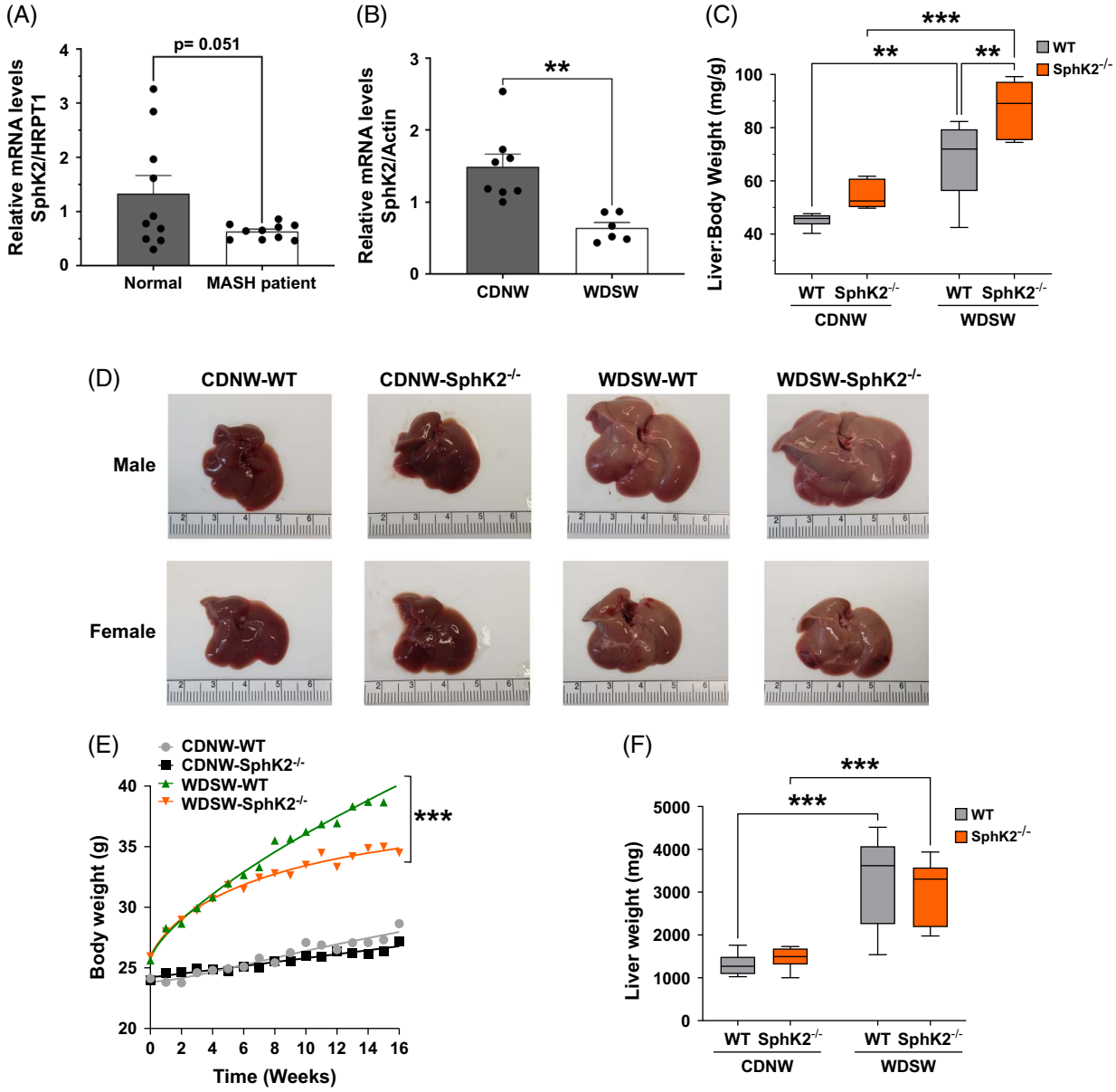

FIGURE 1 SphK2 expression is reduced in MASH and correlates with maintaining liver weight despite body weight loss. (A) Hepatic tissue SphK2 gene expression in patients with MASH (n = 9) and (B) mice fed 16 weeks WDSW (n = 6–8). (C) Liver-to-body weight ratios, (D) liver images, (E) weekly body weights, and (F) terminal liver weights from *SphK2*$^{-/-}$ and WT mice fed 16 weeks CDNW or WDSW. Comparisons of 2 groups were analyzed through a Student unpaired *t* test (A); comparisons of 3 or more groups with 2 independent variables were analyzed through 2-factor ANOVA followed by Sidak MCT for genotype main effects. Values in (A, B) are mean ± SEM of 3–4 independent experiments with 2–3 biological replicates per group; $^{**}p < 0.01$, $^{***}p < 0.001$. Abbreviations: CDNW, control diet plus normal water; MASH, metabolic dysfunction-associated steatohepatitis; MCT, multiple comparisons test; SphK, sphingosine kinase; WDSW, western diet plus sugar water; WT, wild type.

that WDSW-fed *SphK2*$^{-/-}$ mice exhibited increased serum ALT levels compared with CDNW-WT controls (Figure 2C). Serum AST and cholesterol levels were elevated with WDSW feeding in WT and *SphK2*$^{-/-}$ mice, indicating a diet-induced effect (Figure 2D; Supplemental Figure S1A, http://links.lww.com/HC9/B84). Serum triglycerides remained unchanged (Supplemental Figure S1A, http://links.lww.com/HC9/B84). Notably, SphK2 depletion combined with WDSW significantly decreased serum glucose levels to near CDNW controls (Supplemental Figure S1A, http://links.lww.com/HC9/B84). This decrease in terminal blood glucose prompted us to perform intraperitoneal glucose and insulin tolerance tests to determine glucose uptake and clearance as well as insulin sensitivity. However, *SphK2*$^{-/-}$ mice showed only mild or nonsignificant changes in glucose AUC for both the GTT and ITT (Supplemental Figures S1B, C, http://links.lww.com/HC9/B84). These data suggest that reduced SphK2 expression is associated with MASLD disease progression and enhances WDSW-induced liver damage in vivo.

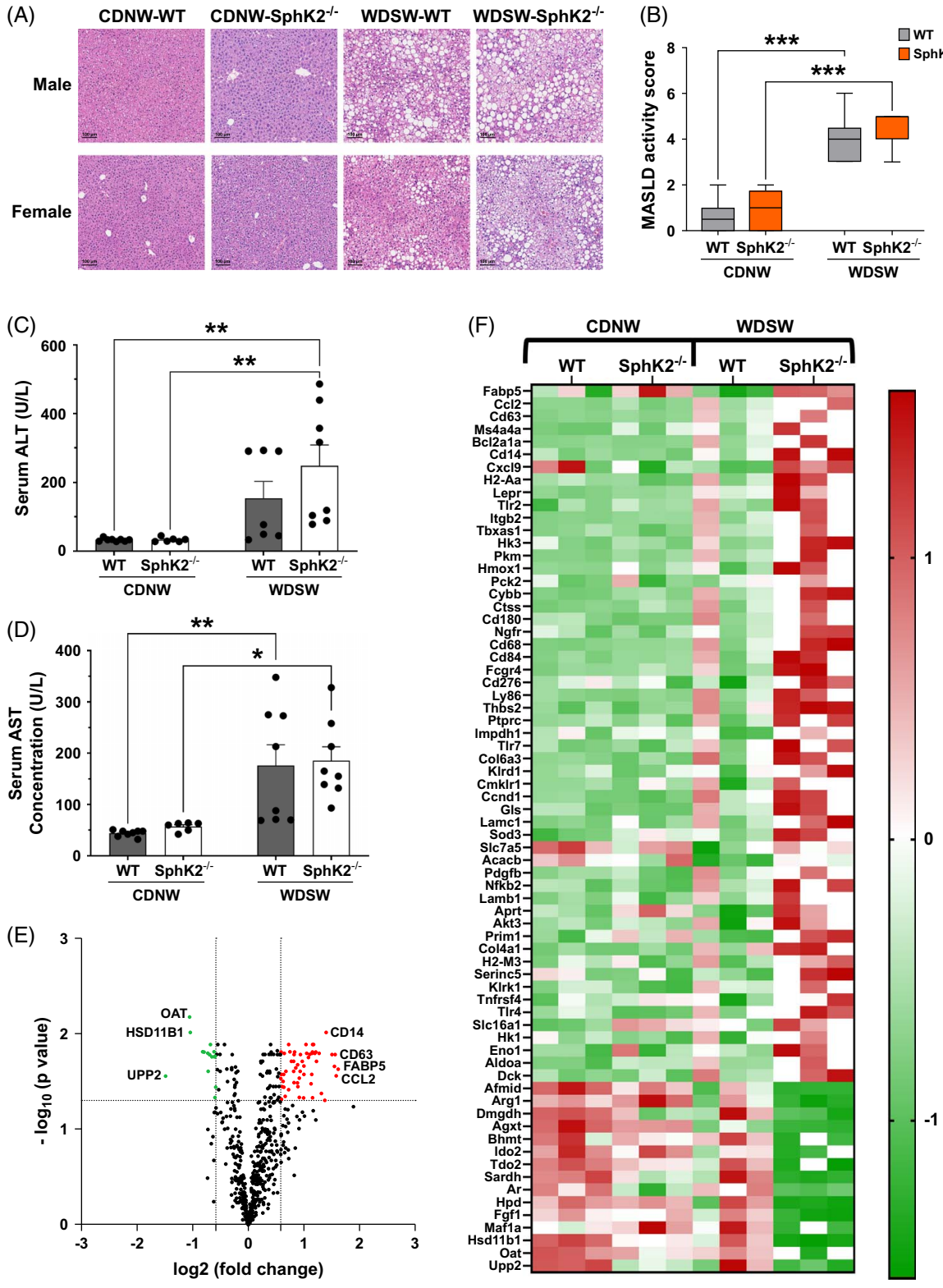

FIGURE 2 SphK2 expression is reduced in MASH and correlates with liver injury. (A) Liver histology by H&E staining and (B) MASLD activity score. (C) Serum ALT and (D) AST serum levels (n = 6–8). (E, F) NanoString nCounter mouse metabolic pathways panel was used to assess gene expression in total RNA isolated from hepatic tissues. (E) Volcano plots from NanoString nCounter data indicate the top genes. (F) All significant genes meet a fold change of ± 2, $p \leq 0.05$. Comparisons of 3 or more groups with 2 independent variables were analyzed through 2-factor ANOVA followed by Sidak MCT. Values in (A, B) are mean ± SEM of 3–4 independent experiments with 2–3 biological replicates per group; $^{*}p < 0.05$, $^{**}p < 0.01$, $^{***}p < 0.001$. Abbreviations: H&E, hematoxylin and eosin; MASH, metabolic dysfunction-associated steatohepatitis; MCT, multiple comparisons test; SphK, sphingosine kinase.

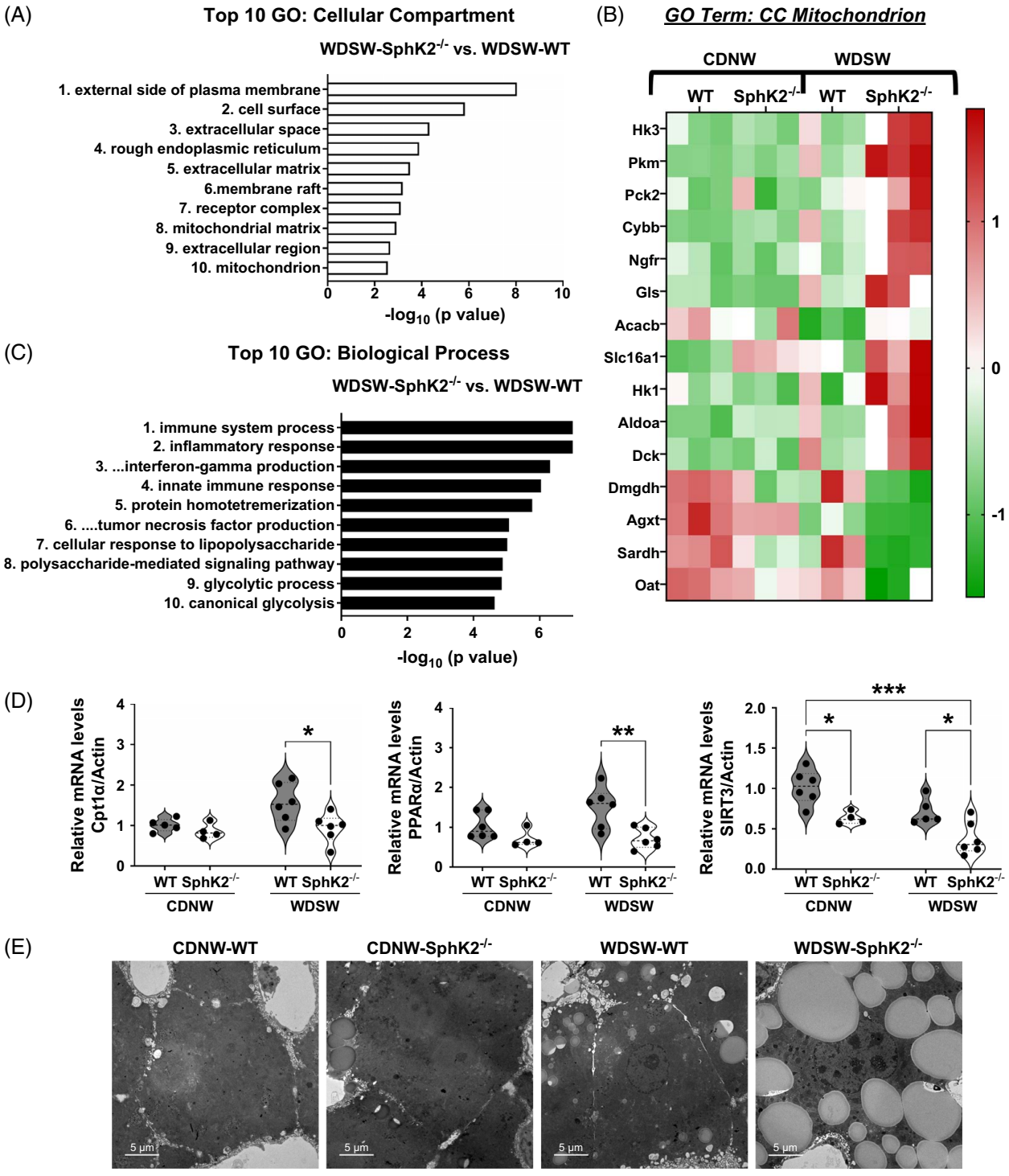

FIGURE 3 SphK2 depletion significantly affects the mitochondrial compartment and increases cellular lipid accumulation. (A) GO for the CC in the NanoString mouse metabolic panel. (B) Corresponding GO heatmap for the CC, Mitochondrion (GO:0005739) in the NanoString mouse metabolic panel. (C) GO for BP in the NanoString mouse metabolic panel (n = 3). (D) *Cpt1a*, *Ppara*, and *SIRT3* expression relative to actin, measured through RT-qPCR (n = 4–6). (E) Transmission electron microscopy images from mouse liver tissue, imaged at ×1500 magnification (CDNW, n = 1; WDSW, n = 2). Comparisons were analyzed through 2-factor ANOVA followed by Sidak MCT. Values in (D) are mean ± SEM of 3–4 independent experiments with 2–3 biological replicates per group; *$p < 0.05$, **$p < 0.01$, ***$p < 0.001$. Abbreviations: BP, biological process; CC, cellular compartment; CDNW, control diet plus normal water; GO, gene ontology; MCT, multiple comparisons test; RT-qPCR, reverse transcription-quantitative polymerase chain reaction; SphK, sphingosine kinase; WDSW, western diet plus sugar water.

SphK2 depletion alters mitochondria-associated gene expression and increases cellular lipid accumulation

To further evaluate SphK2 depletion impacts on hepatic function, we used a NanoString mouse metabolic panel to measure mRNA expression changes in metabolism-associated genes. We identified significant alterations to 70 genes, with 55 upregulated and 15 downregulated genes (fold change ± 2, $p \leq 0.05$). The top upregulated genes included *Cd14*, *Cd63*, *Fabp5*, and *Ccl2*, and the top downregulated genes included *Oat*, *Hsd11b1*, and *Upp2* (Figures 2E, F). Gene ontology (GO) analysis was used to categorize these genes based on shared biological processes (BPs), cellular compartments, and molecular functions. Given our goal to understand SphK2 depletion effects on mitochondrial redox metabolism in MASH, we focused on gene sets related to the mitochondrial compartment. The mitochondrion and mitochondrial matrix were among the top 10 GO cellular compartments identified, and a heatmap was generated to illustrate the significant genes associated with the mitochondrial compartment (Figures 3A, B). Surprisingly, the top 10 GO BP lists for the NanoString mouse metabolic panel were dominated by proinflammatory and immune regulatory gene sets. One of the few metabolic pathways listed among the GO BP was glycolysis (Figure 3C). We also analyzed several genes relevant to mitochondrial beta-oxidation independent of the NanoString panel.[28] *Cpt1α*, *Pparα*, and *Sirt3* were all found to be significantly decreased, and microvesicular steatosis and karyomegaly were observed in the hepatocytes of WDSW-*SphK2*$^{-/-}$ mice compared to WDSW-WT mice (Figures 3D, E).

These findings emphasize that while SphK2 depletion alters hepatic metabolism-related genes, its impact on inflammatory and immune processes predominates the early MASH transcriptional profile. Despite this, SphK2 depletion significantly dysregulates the expression of multiple genes associated with the mitochondrial compartment, underscoring the need for further investigation. Our observed decrease in beta-oxidation–associated genes, paired with increased cellular lipid accumulation, suggests that key mitochondrial processes are dysregulated by SphK2 depletion.

SphK2 depletion alters hepatic mitochondrial composition

Apparent changes in mitochondrial morphology unique to WDSW-*SphK2*$^{-/-}$ mice led us to further investigate SphK2 depletion–induced alterations to mitochondrial composition (Figure 4A). Small particle flow analysis showed a significant increase in mitochondrial size in WDSW-*SphK2*$^{-/-}$ mice compared to CDNW-WT mice (Figure 4B). The key enzymes sterol 27-hydroxylase (CYP27) and cytochrome P450, family 7, subfamily B, polypeptide 1 (CYP7b1) modulate mitochondrial oxysterol levels by determining rates of oxysterol synthesis and hydroxylation, respectively. Oxysterols can affect mitochondrial activity and metabolic processes, multiple signaling cascades, and epigenetic regulation.[20,29,30] Therefore, determining the potential impact of SphK2 depletion on the mitochondrial oxysterol profile is an important consideration in MASH progression. The predominant oxysterols in the mitochondria include cholesterol, 7-dehydroxycholesterol, and lanosterol (Supplemental Figures S2A, B, http://links.lww.com/HC9/B84).

Mitochondrial oxysterol analysis revealed significant elevations in mitochondrial cholesterol (Figure 4C).

We anticipated inhibiting mitochondrial S1P synthesis would significantly alter the hepatic sphingolipid profile. The predominant mitochondrial sphingolipids included C24-1 ceramide (C24-Cer) and C16 sphingomyelin (C16-SM) (Supplemental Figure S3A, http://links.lww.com/HC9/B84). Different sphingolipids were then grouped according to their respective classes. Several sphingolipid intermediates were significantly increased in the hepatic mitochondria of WDSW-*SphK2*$^{-/-}$ compared to WDSW-WT mice, including sphinganine, also referred to as dihydrosphingosine, sphingomyelin (SM), ceramide, and ceramide-1-phosphate (Figures 4D–F). Ceramides have diverse functions; their unique roles are largely attributed to structural differences in chain length.[31] Medium-chain ceramides (C12–C14) visibly increased but were highly variable, which may implicate biological relevance despite their inability to reach statistical significance (Supplemental Figure S3B, http://links.lww.com/HC9/B84). Long-chain ceramides (C16–C20) were significantly increased by SphK2 deletion in WDSW-fed mice. SphK2 depletion, regardless of diet, increased mitochondrial very-long-chain ceramide abundance (C22–C26) (Figure 4E). Mitochondrial ceramide levels were also analyzed separately, revealing that the most abundant and significant elevations were observed in C18:1 and C24:1 ceramide (Supplemental Figures S4A–C, http://links.lww.com/HC9/B84). These data suggest SphK2 depletion increases mitochondrial size, cholesterol, and sphingolipid content, which influences mitochondrial membrane fluidity and overall function.

SphK2 depletion is associated with RC-IV–mediated mitochondrial redox dysfunction and increased hepatic oxylipin abundance

Oxidative phosphorylation involves a series of redox reactions performed by specialized complexes embedded in the inner mitochondrial membrane. As central redox sites, mitochondrial dysfunction can promote broader

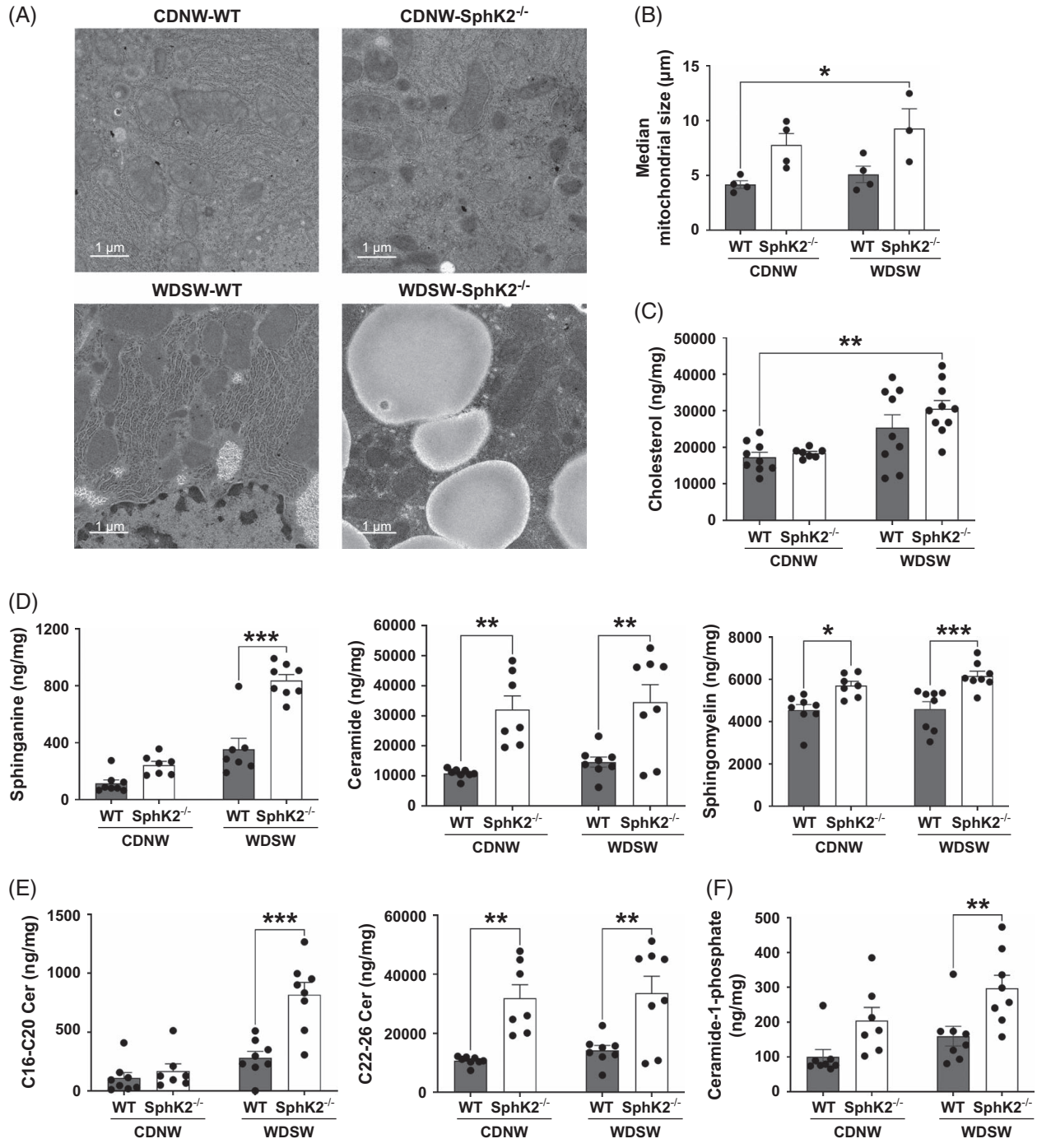

FIGURE 4 SphK2 depletion alters mitochondrial morphology and composition. (A) Transmission electron microscopy images from mouse liver tissue, imaged at ×8000 magnification (CDNW, n = 1; WDSW, n = 2). (B) Small particle flow cytometry for mitochondrial sizes (µm). (C) LC-MS/MS quantification of cholesterol and (D–F) sphingolipids in isolated mitochondrial samples. (E) Ceramides from the same sample set were grouped based on chain length (n = 6–11). Comparisons were analyzed through 2-factor ANOVA followed by Sidak MCT. Values are mean ± SEM of 2–3 independent experiments with 2–4 biological replicates per group; *$p < 0.05$, **$p < 0.01$, ***$p < 0.001$. Abbreviations: CDNW, control diet plus normal water; LC-MS/MS, liquid chromatography and tandem mass spectrometry; MCT, multiple comparisons test; SphK, sphingosine kinase; WDSW, western diet plus sugar water.

redox imbalances at the cellular level.[32] Oxidoreductase activities were among the top molecular functions identified through NanoString, and a heatmap was generated to display the significant genes. The upregulated genes included mostly important oxidases: thromboxane A synthase 1 (*Tbxas1*), heme oxygenase-1 (*Hmox1*), cytochrome b-245, and beta chain (*Cybb*). Downregulated mitochondria redox–associated genes included dimethylglycine dehydrogenase (*Dmgdh*) and sarcosine dehydrogenase (*Sardh*) (Figures 5A, B).

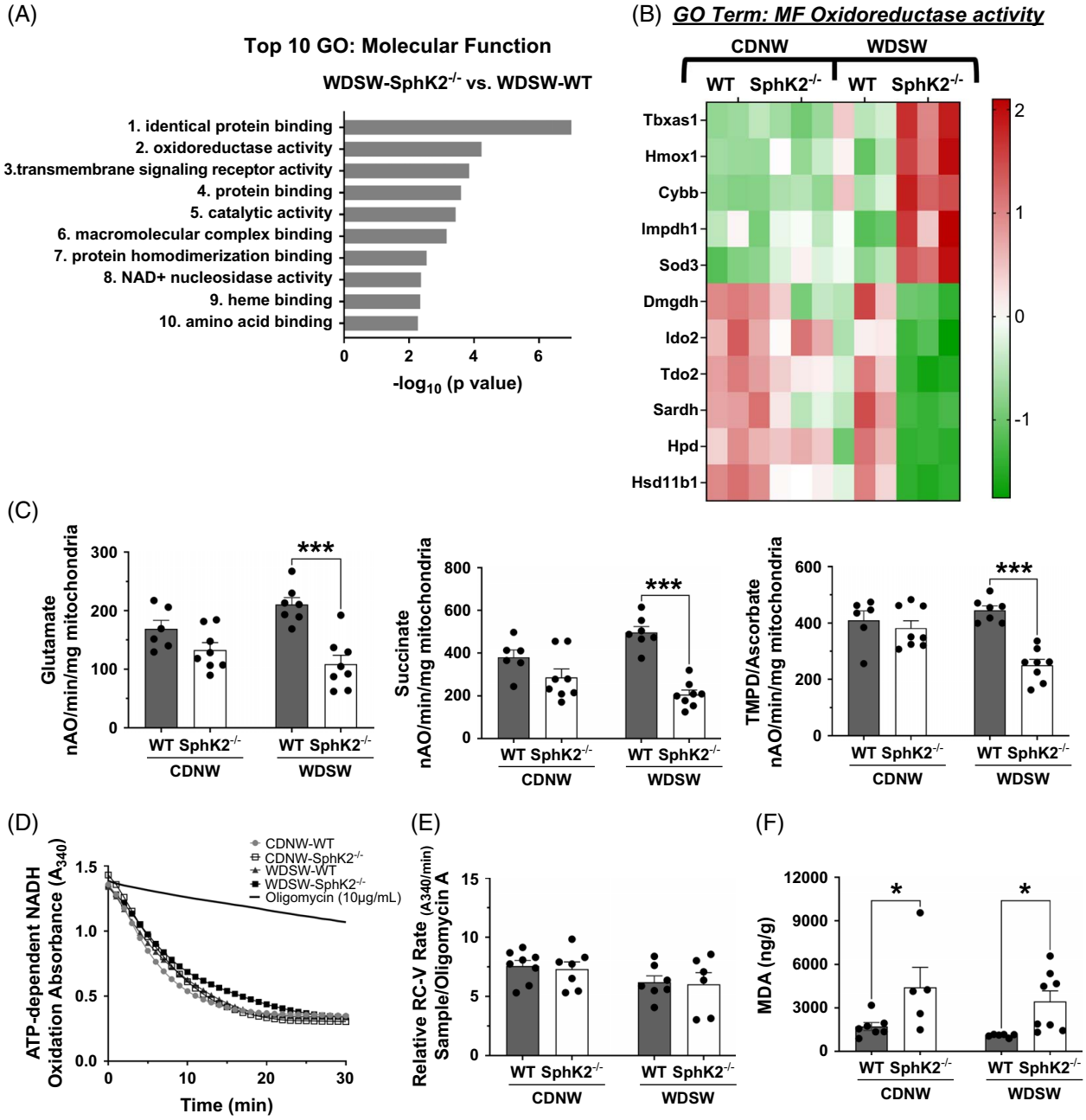

FIGURE 5 SphK2 depletion alters overall cellular redox activity, RC-IV–mediated mitochondrial redox metabolism, and promotes MDA lipid oxidation product formation. (A) GO for MF in the NanoString mouse metabolic panel. (B) Corresponding GO heatmap for MF, Oxidoreductase activity (GO:0016491) (n = 3). (C) Strathkelvin oximeter measurements for maximal ADP-mediated respiration in isolated hepatic mitochondria using the glutamate assay (RC-I to RC-IV), succinate assay (RC-II to RC-IV), and TMPD assay (RC-IV) (n = 6–8). Measurement of RC-V enzyme activity with MitoCheck assay through (D) raw rates and (E) rates relative to oligomycin (n = 6–8). (F) LC-MS/MS quantification of MDA in mouse hepatic tissue (n = 5–8) Comparisons were analyzed through 2-factor ANOVA followed by Sidak MCT. Values are mean ± SEM of 2–3 independent experiments with 2–4 biological replicates per group; *$p < 0.05$, ***$p < 0.001$. Abbreviations: GO, gene ontology; LC-MS/MS, liquid chromatography and tandem mass spectrometry; MCT, multiple comparisons test; MDA, malondialdehyde; MF, molecular function; RC, respiratory complex; SphK, sphingosine kinase; TMPD, tetramethyl-p-phenylene diamine.

To assess the effects of SphK2 depletion on mitochondrial redox metabolism more rigorously, we analyzed hepatic mitochondrial function using a Strathkelvin oximeter with substrates and inhibitors targeting specific RCs (Supplemental Tables S2–S4, http://links.lww.com/HC9/B84). Consistently, we observed a significant reduction in maximal ADP-mediated respiration in coupled mitochondria across RC-I through RC-IV (Figure 5C). The final tetramethyl-p-phenylene diamine/ascorbate test, which supplies electrons directly to RC-IV through cytochrome c reduction, was used to identify potential defects unique to RC-IV function. SphK2

depletion significantly impaired RC-IV function in WDSW-fed mice, suggesting a direct link between SphK2 and its product, S1P, in maintaining RC-IV function. To rule out potential confounding effects on RC-IV function by RC-V, we tested whether RC-V activity was altered by SphK2 depletion. An enzymatic test to assess phosphorylation activity was appropriate since RC-V is not oxygen-dependent. However, direct RC-V enzyme activity measurements revealed no significant differences based on the raw NADH oxidation values or relative to the oligomycin (RC-V inhibitor) background rate (Figures 5D, E). Consistent with these changes in redox metabolism, we found that SphK2 deletion, regardless of diet, resulted in significant increases in hepatic malondialdehyde (MDA), an advanced lipid peroxidation product, and reactive carbonyl aldehyde (Figure 5F). These data suggest that SphK2 depletion dysregulates cellular redox metabolism, which correlates with increased levels of proinflammatory oxylipins, such as MDA, within hepatic tissue.

Hepatic proinflammatory mediators and immune infiltration are increased in SphK2-depleted mice

Previous studies have shown that oxylipins promote inflammation and may participate in both innate and adaptive immune responses in MASH.[33,34] To capture the broad effects of SphK2 depletion on immune-related processes, a mouse immunology NanoString panel was used to compare the immune-associated transcriptional profile in *SphK2*$^{-/-}$ versus WT hepatic tissues in CDNW-fed and WDSW-fed mice. Seventy-five genes were found to be significantly upregulated (71 genes) or downregulated (4 genes) in this panel with a fold change of ± 2, $p \leq 0.05$). Some top upregulated genes included *Bcl6*, *Defb1*, *Ccl6*, and *Il1a*, and the top downregulated genes included *Cd1d1* and *Ctsc* (Figures 6A, B). The GO BP analysis highlighted innate immune response regulation as one of the top processes affected (Figure 6C). Notably, we did not observe an increase in hepatic SphK1 expression in *SphK2*$^{-/-}$ mice (Supplemental S5B, http://links.lww.com/HC9/B84). Since MDA is significantly elevated in the hepatic tissue, which can be formed during arachidonic acid peroxidation, we measured a panel of 30 arachidonic acid metabolites using tandem mass spectrometry (Figure 7A).[32] While SphK2 depletion moderately altered many hepatic eicosanoids, only prostaglandins PGD2, PGF2α, PGE1, and PGE2 were significantly elevated in WDSW-*SphK2*$^{-/-}$ compared to WDSW-WT mice (Figure 7B). MASH is characterized by both inflammation and varying degrees of fibrosis. Sirius red staining showed that SphK2 depletion increased fibrosis compared to WT in WDSW-fed mice (Figures 7C, D).

Detecting multiple proinflammatory mediators led us to further characterize SphK2 depletion on hepatic immune infiltration and activation. We assessed the hepatic immune profile using spectral flow cytometry with a comprehensive panel modified from our previous works (Supplemental Table S6, http://links.lww.com/HC9/B84).[35] SphK2 depletion significantly increased immune cell infiltration into the liver. (Figures 8A, D; Supplemental Figure S5A, http://links.lww.com/HC9/B84). In addition, classical dendritic cells and monocyte-derived macrophages were significantly increased in *SphK2*$^{-/-}$ mouse livers (Figures 8B, C, E, F; Supplemental Figures S5C, D, http://links.lww.com/HC9/B84). In WDSW fed mice, intracellular cytokine staining showed that monocyte-derived macrophages from *SphK2*$^{-/-}$ mice exhibit elevated levels of TNFα compared to WT controls. As determined by intracellular cytokine staining with flow cytometry (Figure 8F). These findings suggest that SphK2 depletion enhances proinflammatory oxylipin formation and augments innate immune responses in an early MASH mouse model.

DISCUSSION

Sphingolipid metabolic dysregulation and mitochondrial dysfunction are well-established contributors to MASLD pathological progression.[4,5,8] S1P receptor 2 and SphK2 are critical lipid metabolic regulators in steatotic liver diseases, including MASLD.[20–23] Previous studies have not fully assessed the combined roles of SphK2 and WDSW in regulating mitochondrial function and gene expression associated with redox metabolism, inflammation, and the immune response.[24] Moreover, previous studies have primarily focused on SphK2 depletion in hepatic steatosis rather than its impacts on MASH progression. Our findings demonstrate that reduced SphK2 levels are associated with mitochondrial structural and functional changes, coupled with disrupted hepatic redox metabolism and enhanced inflammation and immune cell infiltration in a diet-induced early MASH mouse model. Specifically, we showed that SphK2 depletion impairs hepatic mitochondrial redox metabolism by reducing RC-IV–mediated function in oxidative phosphorylation, which has not been shown in a MASH mouse model.

We initially demonstrated SphK2 downregulation in patients with MASH and the WDSW-fed MASH mouse model. The combination of SphK2 depletion and WDSW feeding exacerbated liver injury, as demonstrated by significant elevations in serum ALT, a hepatocellular enzyme released during liver injury.[36] Although SphK2 depletion altered hepatic metabolism

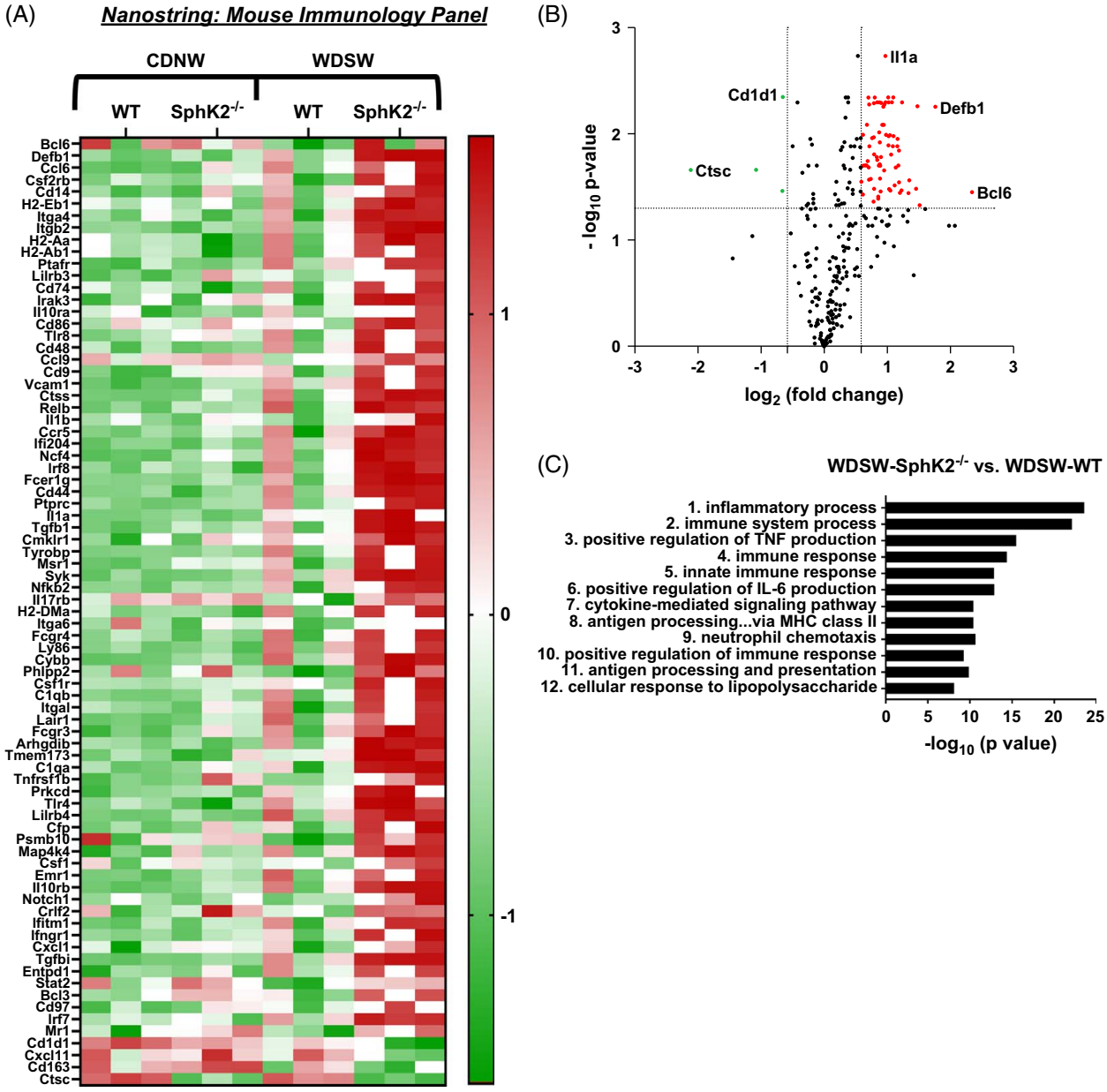

FIGURE 6 SphK2 depletion increases hepatic inflammation. (A) The total hepatic liver RNA of SphK2 KO versus WT mice was used with a NanoString nCounter mouse immunology panel to assess gene expression. (A) The top genes from the NanoString nCounter data are indicated in the volcano plot. (B) Heatmap of all significant genes meeting a fold change of ± 2, $p \leq 0.05$. (C) GO for BP in the NanoString mouse immunology panel ($n = 3$). Comparisons were analyzed through 2-factor ANOVA followed by Sidak MCT. Values are mean $\pm$ SEM of 2 independent experiments with 1–2 biological replicates per group. Abbreviations: BP, biological process; GO, gene ontology; MCT, multiple comparisons test; SphK, sphingosine kinase; WT, wild type.

at the transcriptional level, few genes converged to identify a collective impact on specific metabolic pathways. However, mitochondrial beta-oxidation was likely decreased and this could contribute to the lipid-laden hepatocytes observed in WDSW-*SphK2*$^{-/-}$ mice. Furthermore, SphK2 depletion–induced increases in mitochondrial cholesterol and long-chain or very-long-chain ceramides have been linked to either mitochondrial ROS generation or increased mitochondrial membrane permeability, depending on the disease context.[37–39]

Mitochondria are central redox reaction organelles and the main ROS source in MASLD.[15,40] Moreover, mitochondrial dysfunction initiates changes in cellular signaling and redox metabolism that cannot be appropriately disentangled using reductionist approaches, especially in chronic diseases such as MASLD. We observed changes in the expression of several genes associated with redox dysregulation. *Tbxas1*, *Hmox1*, and *Cybb* were the top upregulated genes. Heme oxygenase-1, encoded by *Hmox1*, is localized in the mitochondria and promotes ROS generation through

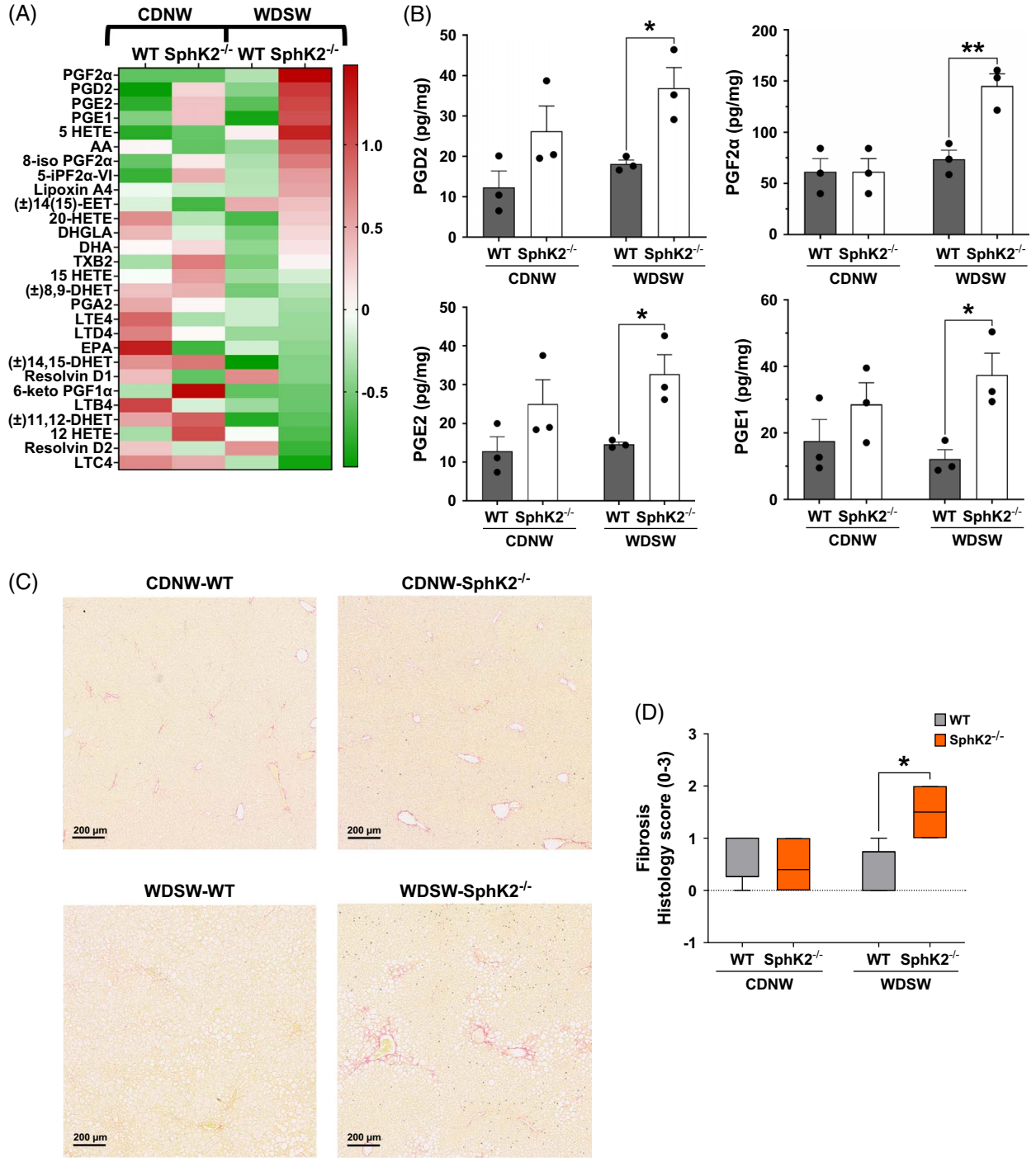

FIGURE 7 SphK2 depletion increases hepatic prostaglandins and fibrosis. (A) LC-MS/MS quantification of arachidonic acid metabolites in mouse hepatic tissue (n = 3). (B) All significant comparisons for arachidonic acid metabolites. (C, D) Sirius red staining of liver tissue and fibrosis scoring. Comparisons were analyzed through 2-factor ANOVA followed by Sidak MCT. Values are mean ± SEM of 2 independent experiments with 1–2 biological replicates per group; *$p < 0.05$, **$p < 0.01$. Abbreviations: LC-MS/MS, liquid chromatography and tandem mass spectrometry; MCT, multiple comparisons test; SphK, sphingosine kinase.

heme catabolism and RC-I function.[41] Consistent with previous findings in cardiomyocytes, SphK2 depletion impedes mitochondrial redox metabolism by significantly reducing RC-IV function, as shown by the reduced respiration incurred in the tetramethyl-p-phenylene diamine test, which bypasses the early RC complexes and supplies electrons directly to RC-IV.[42,43] However, *Dmgdh* and *Sardh* downregulation may also impact mitochondrial redox metabolism by limiting electron availability for coenzyme Q oxidation in the Q cycle of oxidative phosphorylation.[44] These data suggest that SphK2 may exert effects on mitochondrial

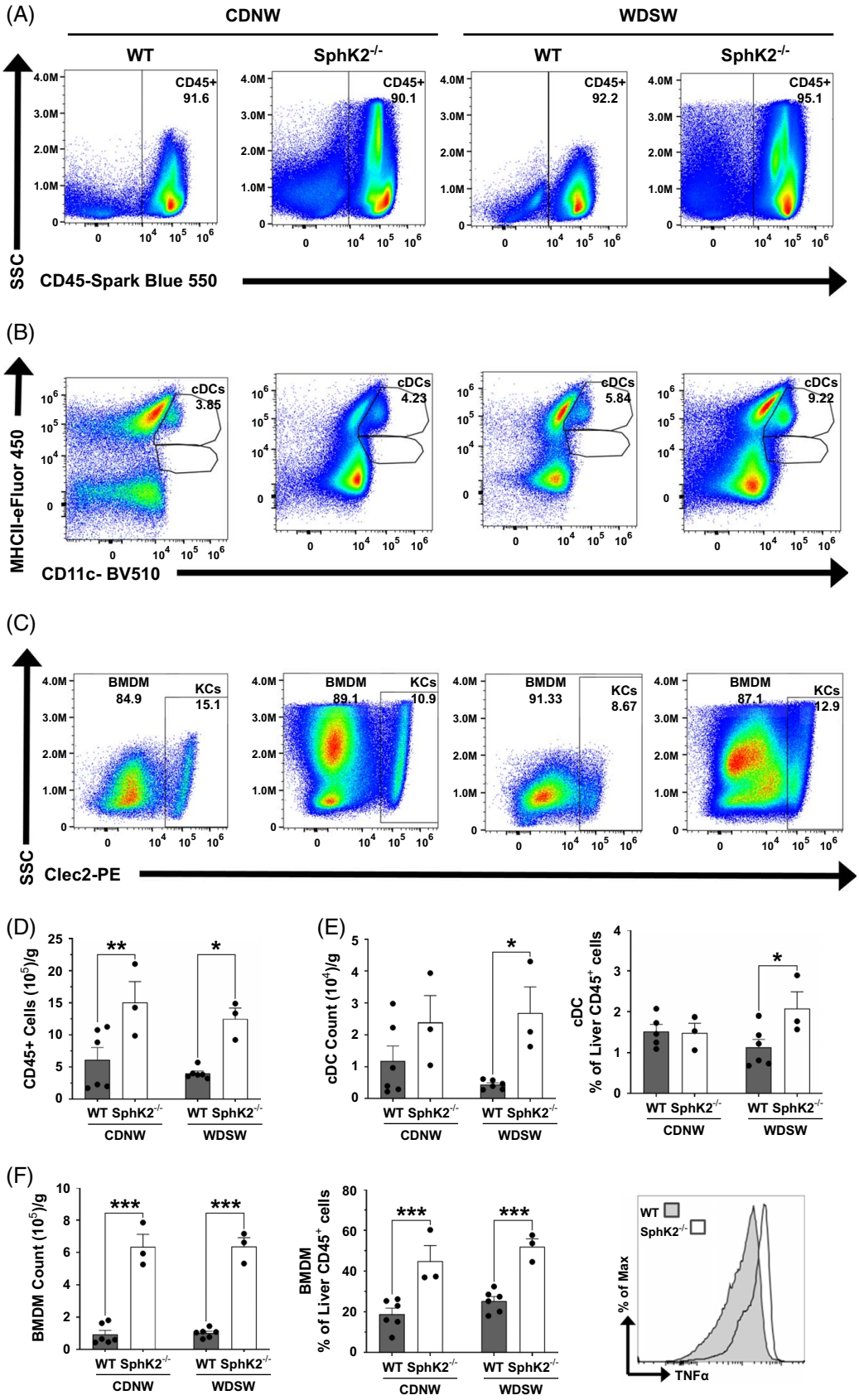
(A)
CDNW
WDSW
WT
SphK2-/-
WT
SphK2-/-
CD45+ 91.6
CD45+ 90.1
CD45+ 92.2
CD45+ 95.1
SSC
CD45-Spark Blue 550
(B)
cDCs 3.85
cDCs 4.23
cDCs 5.84
cDCs 9.22
MHCII-eFluor 450
CD11c- BV510
(C)
BMDM 84.9
KCs 15.1
BMDM 89.1
KCs 10.9
BMDM 91.33
KCs 8.67
BMDM 87.1
KCs 12.9
SSC
Clec2-PE
(D)
CD45+ Cells (10^5)/g
WT SphK2-/-
CDNW
WDSW
(E)
cDC Count (10^4)/g
cDC % of Liver CD45+ cells
(F)
BMDM Count (10^5)/g
BMDM % of Liver CD45+ cells
WT
SphK2-/-
% of Max
TNFα

FIGURE 8 SphK2 depletion increases hepatic immune homing and activation. The immune profile was determined using spectral flow cytometry and normalized by liver mass. Ten million events were collected from whole-liver single-cell suspension and pre-gated for singlet, Zombie-UV$^-$, live lymphocytes. Gating for (A) total immune (CD45$^+$) cell counts, (B) cDCs (pre-gated F4/80$^-$, NK1.1$^-$), and (C) BMDM counts (pre-gated for F4/80$^+$, CD11b$^+$) are displayed. (D) Total cell counts for all CD45+ lymphocytes. (E) cDC (MHCII$^+$, CD11c$^+$) total cell counts and percent of CD45+ cells. (F) BMDM (F4/80$^+$, CD11b$^+$, Tim4$^-$, Clec2$^-$) total cell counts, percent of CD45+ cells, and expression of TNFα based on intracellular cytokine staining via flow. Comparisons were analyzed through 2-factor ANOVA followed by Sidak MCT. Values are mean ± SEM of 2 independent experiments with 1–3 biological replicates per group; $^*p < 0.05$, $^{**}p < 0.01$, $^{***}p < 0.001$. Abbreviations: BMDM, monocyte-derived macrophage; MCT, multiple comparisons test; SphK, sphingosine kinase.

redox metabolism both through the modulation of RC-IV function and gene regulation.

Both mitochondrial and cellular redox dysregulation may contribute to inflammatory progression in WDSW-*SphK2*$^{-/-}$ mice. Alterations in redox metabolism dysregulation co-occurred with significant increases in hepatic MDA synthesis, proinflammatory gene expression, and prostaglandin abundance. MDA and prostaglandins are proinflammatory oxylipins. Increases in MDA levels are most commonly associated with polyunsaturated fatty acid oxidation by ROS.[33] However, the enzyme thromboxane A synthase 1 encoded by the *Tbxas1* gene converts prostaglandin H2 to 12-hydroxy-heptadecatrienoicacid and MDA. Both oxidative species and cyclooxygenase-2 enzyme activity may generate prostaglandins. However, cyclooxygenase-2 may also be regulated by oxidative stress.[45] Similarly, increased *Cybb*, which encodes for gp91-phox, expression may indicate elevated NADPH oxidase activity and be associated with phagocytic activity.[46,47] Concurrent with altered hepatic redox metabolism, we also observed increased proinflammatory cytokine expression and immune infiltrate, including bone marrow–derived macrophages and classical dendritic cells. These data suggest that SphK2 depletion affects multiple aspects of both mitochondrial and overall cellular redox metabolism, which may contribute to proinflammatory mediator production and promote an immune response in the MASH model.

Our current study links SphK2 depletion–mediated redox dysregulation to the generation of oxylipins and other proinflammatory mediators that augment the early immune response in MASH. At the cellular level, decreased SphK2 levels in the mitochondria and nuclear compartments are distinct but likely to participate in reciprocal regulation. Mitochondrial dysfunction alters the overall cellular redox metabolism, inducing transcriptional changes in redox-related genes, such as oxidoreductases. These genes participate in several pathways, including those that generate superoxide and proinflammatory eicosanoids that stimulate hepatic immune infiltration in MASH. This study highlights the critical role of SphK2 in mitochondrial and nuclear regulation within hepatic tissue and demonstrates the potential inflammatory implications of reduced hepatic SphK2 levels in MASLD pathological progression.

AUTHOR CONTRIBUTIONS

Kaitlyn G. Jackson conceived the project, designed the experiments, acquired and analyzed the data, wrote the manuscript, created figures, and prepared the final manuscript for publication. Derrick Zhao assisted with NanoString and obtained the raw data. Lianyong Su ran and processed LC-MS/MS samples. Marissa K. Lipp and Cameron Toler assisted Kaitlyn G. Jackson with experiments. Michael Idowu provided clinical histology scores. Qianhua Yan aided data organization for select supplemental figures. Xuan Wang provided perfusion assistance. Emily Gurley maintained mouse colonies. Huiping Zhou, Phillip B. Hylemon, Jeffrey L. Dupree, Edward J. Lesnefsky, Qun Chen, Puneet Puri, and Nan Wu oversaw project conception, data analysis, and manuscript preparation. All authors critically reviewed the final manuscript and agreed to be accountable for this work.

ACKNOWLEDGMENTS

Services in support of this research project were provided by the VCU Massey Cancer Center Microscopy Core, the VCU Flow Cytometry Shared Resource, the Lipidomics and Metabolomics Shared Resource, and the VCU Massey Comprehensive Cancer Center Tissue and Data Acquisition and Analysis Shared Resource, which were supported, in part, with funding from the NIH-NCI Cancer Center Support Grant, P30 CA016059. The graphical abstract was created using BioRender.com.

FUNDING INFORMATION

This study was supported by (to Huiping Zhou) VA Merit Award 5 I01 BX005730; VA Research Career Scientist (IK6BX004477); VA ShEEP grants (1IS1BX004777-01, 1IS1BX005517-01), National Institutes of Health Grant 2R56DK115377-05A1, 5R01 AA030180, 1R01DK139587-01, 1P01CA275740-01A1, and (Kaitlyn G. Jackson) F31 DK135372.

CONFLICTS OF INTEREST

Michael Idowu consults for Clinnovate UK, PathAI, and Target RWE. The remaining authors have no conflicts to report.

REFERENCES

1. Younossi ZM, Golabi P, Paik JM, Henry A, Van Dongen C, Henry L. The global epidemiology of nonalcoholic fatty liver disease

(NAFLD) and nonalcoholic steatohepatitis (NASH): A systematic review. Hepatology. 2023;77:1335–47.
2. Rohrbach TD, Asgharpour A, Maczis MA, Montefusco D, Cowart LA, Bedossa P, et al. FTY720/fingolimod decreases hepatic steatosis and expression of fatty acid synthase in diet-induced nonalcoholic fatty liver disease in mice. J Lipid Res. 2019;60: 1311–22.
3. Kisseleva T, Brenner D. Molecular and cellular mechanisms of liver fibrosis and its regression. Nat Rev Gastroenterol Hepatol. 2021;18:151–66.
4. Green CD, Maceyka M, Cowart LA, Spiegel S. Sphingolipids in metabolic disease: The good, the bad, and the unknown. Cell Metab. 2021;33:1293–306.
5. Simon J, Ouro A, Ala-Ibanibo L, Presa N, Delgado TC, Martínez-Chantar ML. Sphingolipids in non-alcoholic fatty liver disease and hepatocellular carcinoma: Ceramide turnover. Int J Mol Sci. 2019;21:40.
6. Won JS, Singh I. Sphingolipid signaling and redox regulation. Free Radic Biol Med. 2006;40:1875–88.
7. Nakata R, Hyodo F, Murata M, Eto H, Nakaji T, Kawano T, et al. In vivo redox metabolic imaging of mitochondria assesses disease progression in non-alcoholic steatohepatitis. Sci Rep. 2017;7:17170.
8. Tilg H, Adolph TE, Moschen AR. Multiple parallel hits hypothesis in nonalcoholic fatty liver disease: Revisited after a decade. Hepatology. 2021;73:833–42.
9. Day CP, James OF. Steatohepatitis: A tale of two "hits"? Gastroenterology. 1998;114:842–5.
10. Myint M, Oppedisano F, De Giorgi V, Kim BM, Marincola FM, Alter HJ, et al. Inflammatory signaling in NASH driven by hepatocyte mitochondrial dysfunctions. J Transl Med. 2023;21:757.
11. Koliaki C, Szendroedi J, Kaul K, Jelenik T, Nowotny P, Jankowiak F, et al. Adaptation of hepatic mitochondrial function in humans with non-alcoholic fatty liver is lost in steatohepatitis. Cell Metab. 2015;21:739–46.
12. Jackson KG, Way GW, Zeng J, Lipp MK, Zhou H. The dynamic role of endoplasmic reticulum stress in chronic liver disease. Am J Pathol. 2023;193:1389–99.
13. Corkey BE, Deeney JT. The redox communication network as a regulator of metabolism. Front Physiol. 2020;11:567796.
14. Lennicke C, Cochemé HM. Redox metabolism: ROS as specific molecular regulators of cell signaling and function. Mol Cell. 2021;81:3691–707.
15. Muri J, Kopf M. Redox regulation of immunometabolism. Nat Rev Immunol. 2021;21:363–81.
16. Luukkonen PK, Qadri S, Ahlholm N, Porthan K, Männistö V, Sammalkorpi H, et al. Distinct contributions of metabolic dysfunction and genetic risk factors in the pathogenesis of non-alcoholic fatty liver disease. J Hepatol. 2022; 76:526–35.
17. Spiegel S. Sphingosine-1-phosphate: From insipid lipid to a key regulator. J Biol Chem. 2020;295:3371–84.
18. Igarashi N, Okada T, Hayashi S, Fujita T, Jahangeer S, Nakamura S. Sphingosine kinase 2 is a nuclear protein and inhibits DNA synthesis. J Biol Chem. 2003;278:46832–9.
19. Don AS, Rosen H. A lipid binding domain in sphingosine kinase 2. Biochem Biophys Res Commun. 2009;380:87–92.
20. Jackson KG, Way GW, Zhou H. Bile acids and sphingolipids in non-alcoholic fatty liver disease. Chin Med J (Engl). 2022;135: 1163–71.
21. Nagahashi M, Takabe K, Liu R, Peng K, Wang X, Wang Y, et al. Conjugated bile acid-activated S1P receptor 2 is a key regulator of sphingosine kinase 2 and hepatic gene expression. Hepatology. 2015;61:1216–26.
22. Liu XT, Chung LH, Liu D, Chen J, Huang Y, Teo JD, et al. Ablation of sphingosine kinase 2 suppresses fatty liver-associated hepatocellular carcinoma via downregulation of ceramide transfer protein. Oncogenesis. 2022;11:67.
23. Kwong EK, Liu R, Zhao D, Li X, Zhu W, Wang X, et al. The role of sphingosine kinase 2 in alcoholic liver disease. Dig Liver Dis. 2019;51:1154–63.
24. Hait NC, Allegood J, Maceyka M, Strub GM, Harikumar KB, Singh SK, et al. Regulation of histone acetylation in the nucleus by sphingosine-1-phosphate. Science. 2009;325:1254–7.
25. Diaz Escarcega R, McCullough LD, Tsvetkov AS. The functional role of sphingosine kinase 2. Front Mol Biosci. 2021;8:683767.
26. Asgharpour A, Cazanave SC, Pacana T, Seneshaw M, Vincent R, Banini BA, et al. A diet-induced animal model of non-alcoholic fatty liver disease and hepatocellular cancer. J Hepatol. 2016;65: 579–88.
27. Huby T, Gautier EL. Immune cell-mediated features of non-alcoholic steatohepatitis. Nat Rev Immunol. 2022;22:429–43.
28. Han Y, Zhou S, Coetzee S, Chen A. SIRT4 and its roles in energy and redox metabolism in health, disease and during exercise. Front Physiol. 2019;10:1006.
29. Ren S, Ning Y. Sulfation of 25-hydroxycholesterol regulates lipid metabolism, inflammatory responses, and cell proliferation. Am J Physiol Endocrinol Metab. 2014;306:E123–30.
30. Pandak WM, Kakiyama G. The acidic pathway of bile acid synthesis: Not just an alternative pathway (☆). Liver Res. 2019; 3:88–98.
31. Pinto SN, Silva LC, Futerman AH, Prieto M. Effect of ceramide structure on membrane biophysical properties: The role of acyl chain length and unsaturation. Biochim Biophys Acta. 2011; 1808:2753–60.
32. Marí M, Colell A, Morales A, von Montfort C, Garcia-Ruiz C, Fernández-Checa JC. Redox control of liver function in health and disease. Antioxid Redox Signal. 2010;12:1295–331.
33. Sutti S, Albano E. Adaptive immunity: An emerging player in the progression of NAFLD. Nat Rev Gastroenterol Hepatol. 2020;17: 81–92.
34. Hendrikx T, Binder CJ. Oxidation-specific epitopes in non-alcoholic fatty liver disease. Front Endocrinol (Lausanne). 2020;11:607011.
35. Way GW, Lu H, Wang X, Zhao D, Camarena C, Sarkar D, et al. Optimization of high throughput spectral flow cytometry for immune cell profiling in mouse liver. Liver Res. 2023;7:263–71.
36. Kim WR, Flamm SL, Di Bisceglie AM, Bodenheimer HC. Serum activity of alanine aminotransferase (ALT) as an indicator of health and disease. Hepatology. 2008;47:1363–70.
37. Law BA, Liao X, Moore KS, Southard A, Roddy P, Ji R, et al. Lipotoxic very-long-chain ceramides cause mitochondrial dysfunction, oxidative stress, and cell death in cardiomyocytes. Faseb J. 2018;32:1403–16.
38. Novgorodov SA, Gudz TI, Obeid LM. Long-chain ceramide is a potent inhibitor of the mitochondrial permeability transition pore. J Biol Chem. 2008;283:24707–17.
39. Goicoechea L, Conde de la Rosa L, Torres S, García-Ruiz C, Fernández-Checa JC. Mitochondrial cholesterol: Metabolism and impact on redox biology and disease. Redox Biol. 2023; 61:102643.
40. Handy DE, Loscalzo J. Redox regulation of mitochondrial function. Antioxid Redox Signal. 2012;16:1323–67.
41. Bansal S, Biswas G, Avadhani NG. Mitochondria-targeted heme oxygenase-1 induces oxidative stress and mitochondrial dysfunction in macrophages, kidney fibroblasts and in chronic alcohol hepatotoxicity. Redox Biol. 2014;2:273–83.
42. Salabei JK, Gibb AA, Hill BG. Comprehensive measurement of respiratory activity in permeabilized cells using extracellular flux analysis. Nat Protoc. 2014;9:421–38.
43. Strub GM, Paillard M, Liang J, Gomez L, Allegood JC, Hait NC, et al. Sphingosine-1-phosphate produced by sphingosine kinase 2 in mitochondria interacts with prohibitin 2 to regulate complex IV assembly and respiration. FASEB J. 2011;25:600–12.
44. Herrero Martín JC, Salegi Ansa B, Álvarez-Rivera G, Domínguez-Zorita S, Rodríguez-Pombo P, Pérez B, et al. An ETFDH-driven

metabolon supports OXPHOS efficiency in skeletal muscle by regulating coenzyme Q homeostasis. Nat Metab. 2024;6:209–25.
45. Alric L, Orfila C, Carrere N, Beraud M, Carrera G, Lepert JC, et al. Reactive oxygen intermediates and eicosanoid production by Kupffer cells and infiltrated macrophages in acute and chronic liver injury induced in rats by CCl4. Inflamm Res. 2000;49:700–7.
46. Delli Bovi AP, Marciano F, Mandato C, Siano MA, Savoia M, Vajro P. Oxidative stress in non-alcoholic fatty liver disease. An updated mini review. Front Med (Lausanne). 2021;8:595371.
47. Guilliams M, Scott CL. Liver macrophages in health and disease. Immunity. 2022;55:1515–29.

How to cite this article: Jackson KG, Zhao D, Su L, Lipp MK, Toler C, Idowu M, et al. Sphingosine kinase 2 (SphK2) depletion alters redox metabolism and enhances inflammation in a diet-induced MASH mouse model. Hepatol Commun. 2024;8: e0570. https://doi.org/10.1097/HC9.0000000000000570